The effect of T-atom ratio and TPAOH concentration on the pore structure and titanium position in MFI-Type Titanosilicate during dissolution-recrystallization process

Yilai Jiao,[a, b, †,*] Abdul-Lateef Adedigba,[b, c,†] Nicholas F. Dummer,[b] Jinmin Liu,[a] Yangtao Zhou,[a] Yanan Guan,[a] Hengyu Shen,[a] Micheal Perdjon,[b] Graham J Hutchings* [b]

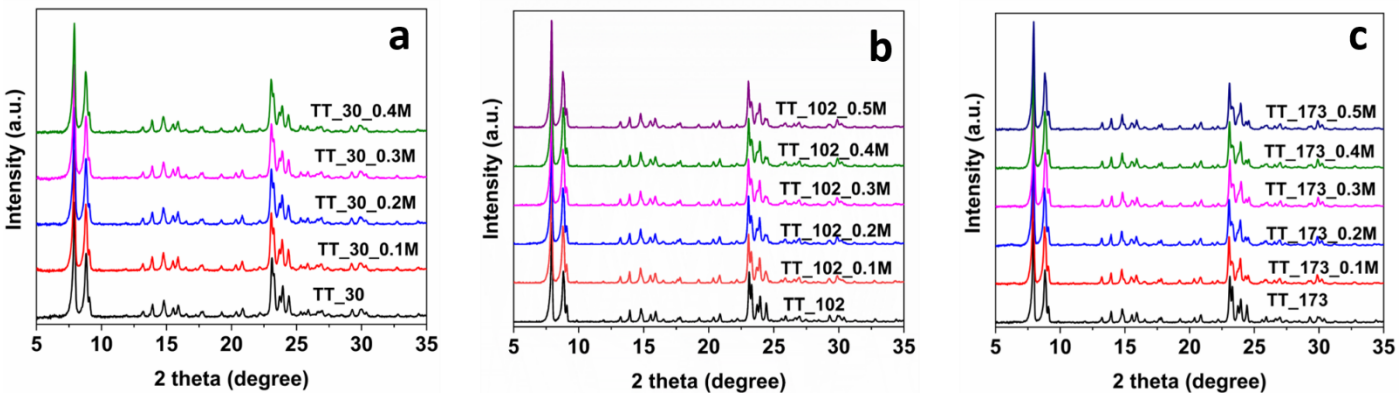

Fig. S1: Full range X-ray powder diffraction patterns of (a) TT_30, (b) TT_102, (c) TT_173 series samples

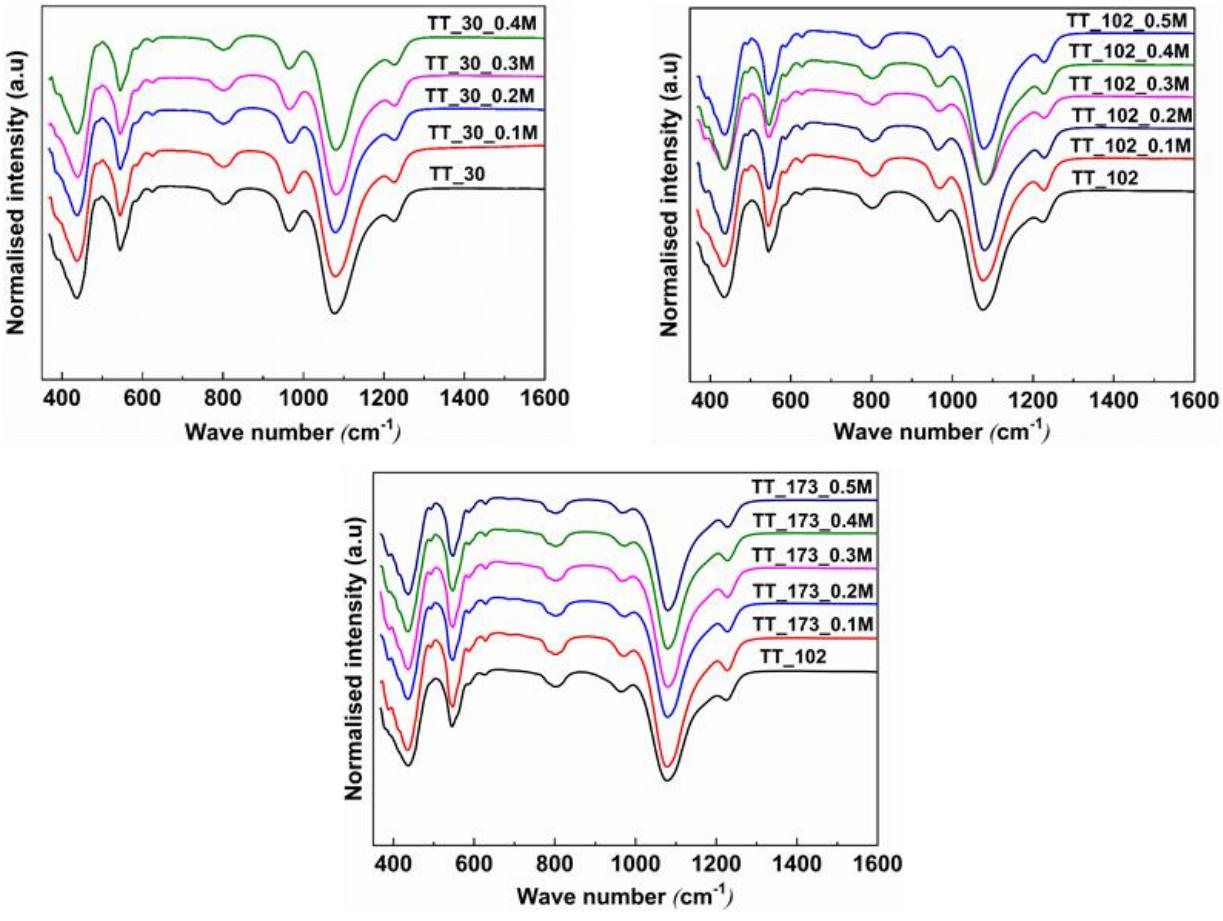

Fig S2: FTIR spectra of as-prepared and TPAOH modified samples

Table S1. Peak deconvolutions of as-prepared and TPAOH modified samples using the PeakFit program with the Gaussian fitting method

Sample	I_{center}	II_{center}	I_{area}	II_{area}
TS_30_AP	203	294	85.6	14.4
TS_30_0.05M	204	293	72	28
TS_30_0.1M	206	292	71.2	28.8
TS_30_0.2M	208	296	77.1	22.9
TS_30_0.3M	211	298	83	17
TS_30_0.4M	211	299	81.5	18.5
TS_102_AP	204	-	100	-
TS_102_0.1M	202	298	84.3	15.7
TS_102_0.2M	193	303	72	28
TS_102_0.3M	192	302	68.8	31.2
TS_102_0.4M	194	302	69.3	30.7
TS_102_0.5M	204	305	66.9	33.1
TS_173	204	-	100	-
TS_173_0.1M	194	303	71.1	28.9
TS_173_0.2M	191	303	67.7	32.3
TS_173_0.3M	192	302	68.8	31.2
TS_173_0.4M	191	304	66.9	33.1
TS_173_0.5M	177	304	68.3	31.7

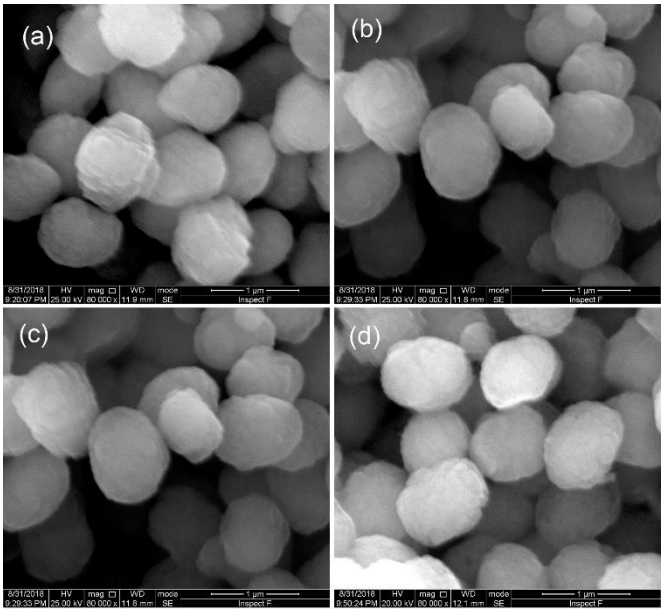

Fig. S3: SEM morphology of TT_30 (a), TT_30_0.2M (b), TT_30_0.3M (c) and TT_30_0.4M (d)

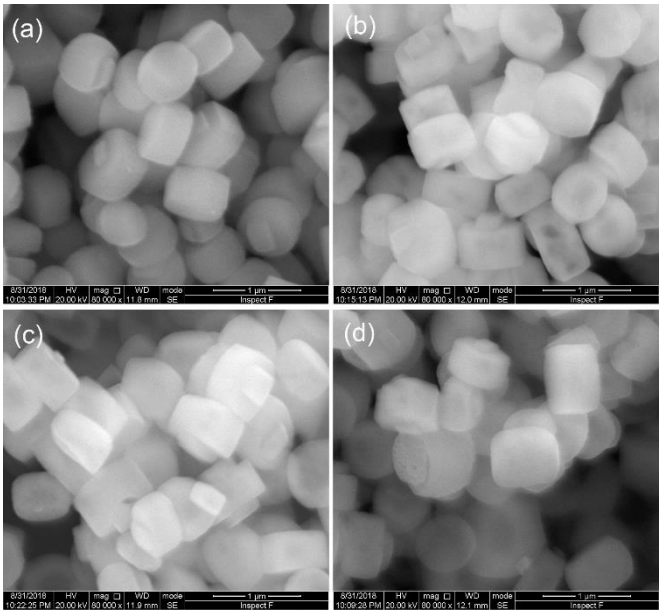

Fig. S4: SEM morphology of TT_102 (a), TT_102_0.2M (b), TT_102_0.4M (c) and TT_102_0.5M (d)

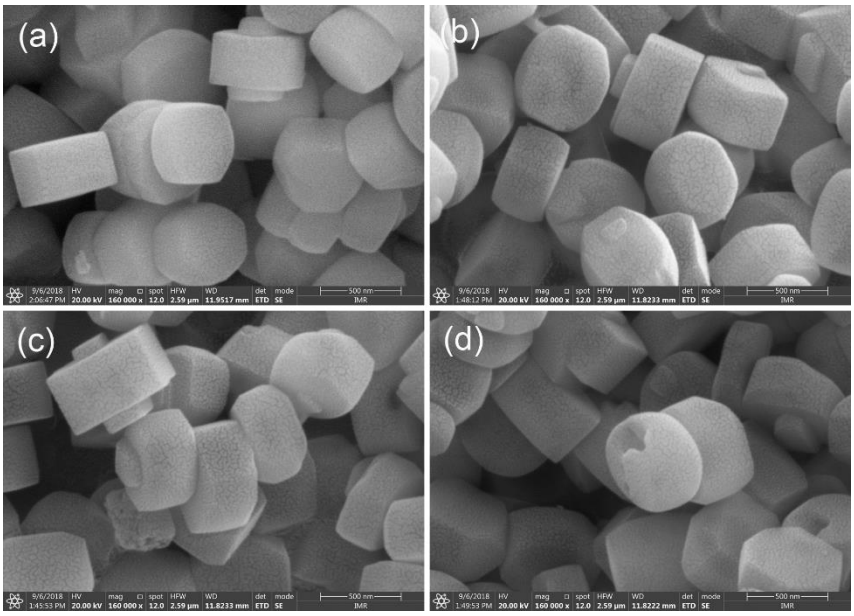

Fig. S5: SEM morphology of TT_173 (a), TT_173_0.2M (b), TT_173_0.4M (c) and TT_173_0.5M (d)

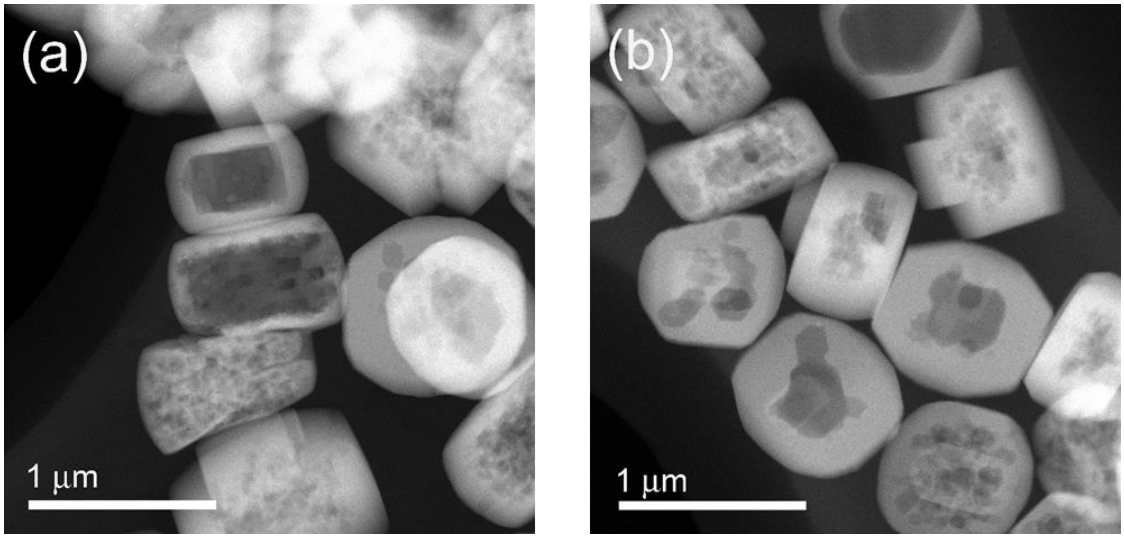

Fig. S6: HAADF morphology of TT_102_0.5M (a) and TT_173_0.5M (b)